International Journal of Latest Engineering Research and Applications (IJLERA) ISSN: 2455-7137

Volume – 03, Issue – 02, February 2018, PP – 34-46

Modified Reynold’s equation for cosine form convex curved plates with porosity and MHD

Syed Arishiya Naseem Fatima[1], Trimbak Biradar[2]

[1] *Department of Mathematics, K.C.T College of Engineering , Gulbarga, India.*

[2] *Department of Mathematics, Sharnbasveshwar College of science, Gulbarga, India.*

Abstract: The surface roughness effect on the magnetohydrodynamic (MHD) lubrication of porous cosine form convex curved plates is presented in this paper. The generalized stochastic Reynold’s equation leading fluid film pressure is obtained for one-dimensional roughness structure. Pressure, load capacity and squeeze film time for modified equations are derived. The calculated values of pressure, load capacity and squeeze film time are displayed in the form of graph. It is seen that extreme permeability of the porous layer causes a considerable fall in the squeeze film characteristics and minimizes surface roughness effect. For transverse roughness case increment in load-carrying capacity and squeeze time is observed when permeability is limited or absent, whereas reverse results are observed for longitudinal roughness case.

Keywords: convex curved plates, cosine function , Magnetic field, porous medium ,surface roughness, squeeze film.

1. Introduction

The magnetic field has vital applications in the industry with apparent relevance to technology-based world. Magnetohydrodynamic (MHD) fluid flow in lubrication of squeeze film prevents the unpredicted deviation of lubricant viscosity with temperature under severe working conditions. Study between curved squeeze film surfaces is carried out by many authors [1-9].The MHD lubrication in an outwardly under pressure thrust bearing has been investigated both hypothetically and experimentally by Maki et al. [10]. Limited studies of MHD lubrication are available in the literature which includes MHD slider bearings [11, 12], MHD journal bearings [13, 14] and MHD squeeze film bearings [15]. Hamza [16] has shown the MHD effects on a fluid film squeezed between two revolving surfaces. Bujurke and Kudenatti [17] have theoretically explored the roughness effect on electrically conducting fluid between two rectangular plates in which an upper plate has a roughness structure.

For self-lubricating porous bearings continuous lubrication is not essential because of their self-sufficient oil reservoir. Lubricating fluid is stored by the interconnecting pores of most of the porous bearings. On applying the load, through these interconnected pores the fluid is supplied to the fluid film area to support the load, and on load removal fluid re-absorbtion is carried out. Porous bearings have wide applications because of their longer period work without extra lubricant where re-lubrication would be difficult. Thus these bearings have been used in vehicle manufacturing, home appliances, machines, and so forth. Because of the importance of porous bearings, Wu [18] studied the squeeze film effects between two rectangular plates in which both plates have a porous material. Different types of porous bearing papers are available for example, journal bearings [19], slider bearings [20], thrust bearings [21] and many more. Naduvinamani et al. [22] have undertaken a detailed study of magnetic effects in rectangular plates and reported that bearing characteristics seems to increase for increasing the Hartman number.

The roughness effect becomes more important for minor gap of mating surfaces. Study on surface roughness is required for better performance of hydrodynamic lubrication in different bearings. Therefore, on this we have various theories by, Christensen [23], Christensen and Tonder [24], and Chow and Cheng [25] within the framework of the stochastic theory, but their studies were restricted to two-dimensional roughness patterns. Later, Patir and Cheng [26] considered the flow between rough surfaces in which the flow is equated to an averaged flow between two smooth surfaces, and the roughness parameter is included directly in the Reynolds equation. However, this approach fails when the random roughness structures are not identical. Christensen’s [23] stochastic model which assumes that the probability density function for the random variable characterizing the roughness is symmetric with the mean of the random variable equal to zero. Christensen’s model shows two types of roughness pattern in the roughness theory. The Reynolds equation which is derived to incorporate roughness structure necessarily includes one dimensional longitudinal and transverse roughness structures. In case of rectangular geometry, only one of the above two cases has been studied (longitudinal case in particular) because the other one can be obtained by just coordinating transformation. Because of this considerable transformation, many theories have been studied in the literature. Bujurke and Naduvinamani [27] derived Reynold's equation for rectangular plates with porosity. This work shows roughness effect is to increase the load capacity of the bearing compared to smooth case.

To the author's knowledge, no investigation is done on effect of roughness and porosity on hydrodynamic lubrication between cosine form of convex curved plates in the presence of transverse magnetic field.

The presentation of the paper proceeds as follows. In second section, with suitable boundary conditions in the fluid film and porous area basic MHD equations are given.The modified Reynolds equation in non-dimensional form is derived from leading equations. Third section discusses the pressure distribution, load-carrying capacity, and squeezing time, important results and so forth. Last section sums up the main ideas and their efficacy in design bearings.

2. Mathematical Formulation of the Problem

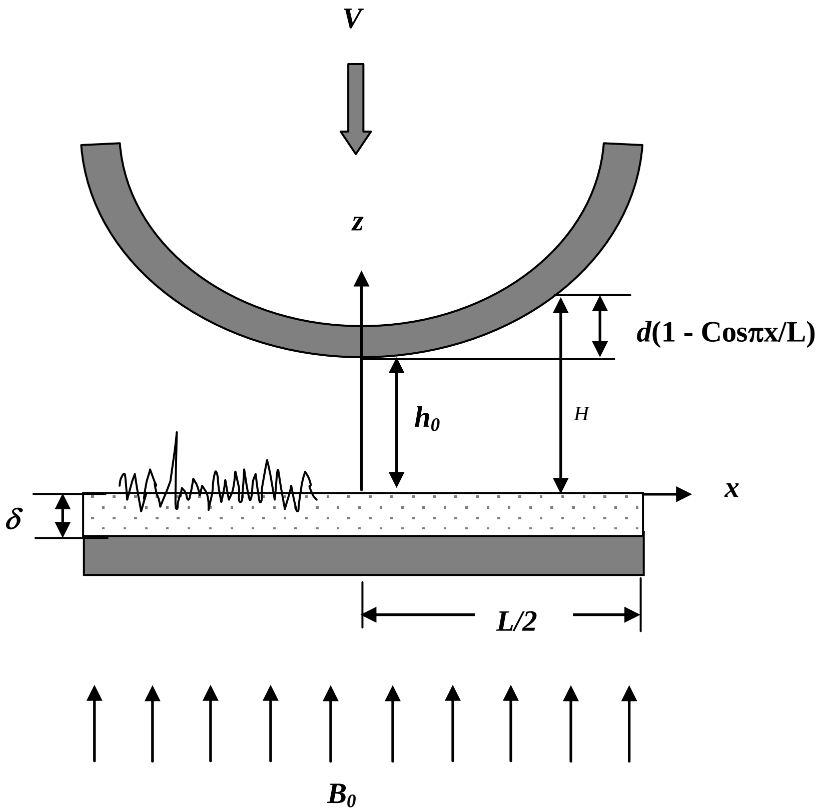

Figure 1: The physical configuration of porous and rough cosine form convex curved plates in the presence of transverse magnetic field.

The geometry of squeeze film between rough and porous cosine form convex curved plates is shown in fig.1. The thickness of the film H is given by the cosine function form $H = h_0 + d\left\{1 - \cos\left(\frac{\pi}{L}x\right)\right\}$ in which L represents length of the plates, d is cosine function amplitude and h_0 is the least thickness of the film. The thickness of the film is equal to the least film thickness at the mid position: $x = 0$ and at the boundary : $x = \frac{L}{2}$, the film thickness is equal to the summation of the least film thickness and the amplitude $h_0 + d$. The above equation is useful to produce different sizes of convex curved surfaces by changing the amplitude's value for the cosine function for a fixed length *L*.

It is supposed that the fluid film is thin hence the body forces and the body couples are insignificant. Under these supposition, the thin film's hydrodynamic lubrication theory , the equation of continuity and the MHD governing equations of motion in cartesian coordinate are

$$:\frac{\partial^2 u}{\partial z^2} - M_0{}^2 u = \frac{1}{\mu}\frac{\partial p}{\partial x} \tag{1}$$

$$:\frac{\partial p}{\partial z} = 0 \tag{2}$$

$$:\frac{\partial u}{\partial x} + \frac{\partial w}{\partial z} = 0 \tag{3}$$

Where $M_0 = \frac{M}{h_0}$ and $M = B_0 h_0 (\frac{\sigma}{\mu})^{1/2}$ is the Hartmann number.

where u is the component of velocity, p is pressure of the film, μ is viscosity of the lubricant, σ is the lubricant's conductivity and applied magnetic field to the bearing in the z -direction is given by B_0 as shown in the fig. 1.

The appropriate boundary conditions for the component of velocity are

i) At the upper surface $z = H$

$$:u = 0(no\ slip) \qquad w = V = \frac{\partial H}{\partial t} \tag{4}$$

ii) At the lower surface $z = 0$

$$:u = 0(no\ slip) \qquad w = w^* \tag{5}$$

Where $\frac{\partial H}{\partial t}$ is an impending velocity of the upper plate to the lower plate and w^* is the modified Darcy velocity component in the $z-$direction in the porous area. Modified form of the Darcy law for porous material is given by

$$:u^* = -\frac{k}{\mu\left(1+\frac{kM_0{}^2}{m}\right)}\frac{\partial p^*}{\partial x} \tag{6}$$

$$:w^* = -\frac{k}{\mu}\frac{\partial p^*}{\partial z} \tag{7}$$

where k is porous matrix permeability, m porosity and p^* is the porous area pressure.

The solution of equation (1) subject to the boundary conditions eqns. (4) and (5) is given by

$$:u = \frac{1}{\mu M_0{}^2}\frac{\partial p}{\partial x}\frac{2\sinh\frac{M_0 z}{2}\sinh\frac{M_0(z-H)}{2}}{\cosh\frac{M_0 H}{2}} \tag{8}$$

Taking u value in the integral form of continuity equation

$$:\frac{\partial}{\partial x}\left\{\int_0^H u\,dz\right\} + w_H - w_0 = 0 \tag{9}$$

in the following continuity equation for lower porous area substituting equations (6) and (7)

$$:\frac{\partial u^*}{\partial x} + \frac{\partial w^*}{\partial z} = 0 \tag{10}$$

Integrating above equation once with respect to z from $-\delta$ to 0 and using the Morgan-Cameron approximation with the condition $\partial p^*/\partial z = 0$ when $z = -\delta$ gives

$$\left(\frac{\partial p^*}{\partial z}\right)_{z=0} = -\frac{\delta}{D}\frac{\partial^2 p}{\partial x^2} \tag{11}$$

where $D = \left(1 + \frac{kM_0{}^2}{m}\right)$ and δ is the porous layer thickness.

Substituting (8) and (11) in (9) gives

$$\frac{\partial}{\partial x}\left\{\frac{\partial p}{\partial x} f\left(H, M_0, k, D\right)\right\} = -V \tag{12}$$

Where $f\left(H, M_0, k, D\right) = \frac{1}{\mu M_0{}^3}\left(M_0 H - 2tanh\frac{M_0 H}{2}\right) + \frac{k\delta}{\mu D}$

For the surface roughness to be mathematically modelled, the fluid film thickness H is made up of two parts $H = h(t) + h_s(x,z,\xi)$ where $h(t)$ is the height of the nominal smooth part of the fluid film region and $h_s(x,z,\xi)$ is the part due to the surface asperities measured from the nominal level and is a randomly varying quantity of zero mean, and ξ is the index parameter determining a definite roughness structure. Let $f(h_s)$ be the probability density function of the stochastic film thickness h_s. Taking the stochastic average of (12) with respect to $f(h_s)$ the averaged modified Reynold's type equation is obtained in the form

$$\frac{\partial}{\partial x}\left\{E\left(f\left(H, M_0, k, D\right)\right)\frac{\partial E(p)}{\partial x}\right\} = -\frac{dH}{dt} \tag{13}$$

Where $E(*)$ denotes the expectancy operator defined by

$$E(*) = \int_{-\infty}^{\infty} (*) f(h_s) dh_s \tag{14}$$

In accordance with Christensen[23], we assume that

$$f(h_s) = \begin{cases} \frac{35}{32c^7}(c^2 - h_s^2)^3 & -c < h_s < c \\ 0 & elsewhere \end{cases} \tag{15}$$

where $\sigma = \frac{c}{3}$ is the standard deviation.

In context of Christensen stochastic theory for the hydrodynamic lubrication of rough surfaces, two types of one-dimensional surface roughness patterns are considered, namely, longitudinal roughness pattern and transverse roughness pattern.

2.1. Longitudinal Roughness Pattern

For the one-dimensional longitudinal roughness pattern, the striations are in the type of long narrow ridges furthermore valleys running in the $x-$direction. In this instance those non- dimensional stochastic film thickness accepts the expression

$H^* = h^* + h_s^*(z,\xi)$. And

the stochastic modified Reynold's equation (13) takes the form

$$\frac{\partial}{\partial x}\left\{E\left(f\left(H, M_0, k, D\right)\right)\frac{\partial E\left(P\right)}{\partial x}\right\} = -\frac{dH}{dt} \tag{16}$$

2.2. Transverse Roughness Pattern

For the particular case one dimensional transverse roughness, the structure need those type of long, narrow ridges also valleys running in the $z-$direction. In this instance those non-dimensional stochastic film thickness expects the form

$H^* = h^* + h_s^*(x,\xi)$.

And the stochastic changed Reynolds equation (13) takes the type

$$:\frac{\partial}{\partial x}\left[\frac{\partial E(p)}{\partial x}\frac{1}{E\left(\frac{1}{f(H,M_0,k,D)}\right)}\right]=-\frac{dH}{dt} \quad (17)$$

Equations (16) and (17) together can be written as

$$:\frac{\partial}{\partial x}\left[\frac{\partial E(p)}{\partial x}G\left(H,M_0,k,D\right)\right]=-\frac{dH}{dt} \quad (18)$$

where $G(H,M_0,k,D)=\begin{cases}E(f(H,M_0,k,D)) & \text{for longitudinal roughness}\\ \{E(1/(f(H,M_0,k,D)))\}^{-1} & \text{for transeverse roughness}\end{cases}$

$$:E(f(H,M_0,k,D))=\frac{35}{32c^7}\int_{-c}^{c}f(H,M_0,k,D)(c^2-h_s^2)^3dh_s \quad (19)$$

$$:E\left(\frac{1}{f(H,M_0,k,D)}\right)=\frac{35}{32c^7}\int_{-c}^{c}\frac{(c^2-h_s^2)^3}{f(H,M_0,k,D)}dh_s \quad (20)$$

Introducing the dimensionless quantities:

$$x^*=\frac{x}{L},H^*=\frac{H}{h_0},p^*=\frac{E(p)h_0^3}{\mu L^2(-dH/dt)},A=\frac{d}{h_0},\psi=\frac{k\delta}{h_0^3},C=\frac{c}{h_0},\delta^*=\frac{\delta}{h_0}$$

Eq. (18) takes the form

$$:\frac{\partial}{\partial x^*}\left\{\frac{\partial p^*}{\partial x^*}G(H^*,M_0,\psi,D)\right\}=-1 \quad (21)$$

$$G(H^*,M_0,\psi,D)=\begin{cases}E(F(H^*,M_0,\psi,D)) & \text{For } \textit{longitudinal} \text{ roughness}\\ \{E(1/(F(H^*,M_0,\psi,D)))\}^{-1} & \text{For } \textit{transverse} \text{ roughness}\end{cases}$$

Where $F(H^*,M_0,\psi,D)=\frac{1}{{M_0}^3}\left(M_0H^*-2tanh\frac{M_0H^*}{2}\right)+\frac{\psi}{D}$,

$D=\left(1+\frac{\psi M_0^2}{m\delta^*}\right)$ and $H^*=1+A\{1-\cos(\pi x^*)\}$.

The pressure conditions are: $P^*=0$ at $x^*=\pm\frac{1}{2}$ and $\frac{dP^*}{dx^*}=0$ at $x^*=0$.

Integration of equation (21) using pressure conditions gives

$$:P^*=-\int_{1/2}^{x^*}\frac{x^*}{G(H^*,M_0,\psi,D)}dx^*$$

$$:P^*=\int_{x^*}^{1/2}\frac{x^*}{G(H^*,M_0,\psi,D)}dx^* \quad (22)$$

By integrating the film pressure, load-carrying capacity can be obtained

$$:W=b\int_{-L/2}^{L/2}pdx$$

Where b represents curved plates width. Introducing dimensionless form gives

$$:W^*=\frac{h_0^3W}{\mu L^3b(-dH/dt)}=\int_{-1/2}^{1/2}P^*dx^* \quad (23)$$

i.e, dimensionless load capacity

$$:W^{*}=\int_{-1/2}^{1/2}\left\{\int_{x^{*}}^{1/2}\frac{x^{*}}{G(H^{*},M_{0},\psi,D)}dx^{*}\right\}dx^{*} \tag{24}$$

Introducing non-dimensional time as

$$:T^{*}=\frac{Wh_{0}^{2}t}{\mu L^{3}b}$$

The elapsed time need for the upper curved plate to move towards the lower plate is given by

$$:T^{*}=\int_{h_{0}^{*}}^{1}\left[\int_{-1/2}^{1/2}\left\{\int_{x^{*}}^{1/2}\frac{x^{*}}{G(H^{*},M_{0},\psi,D)}dx^{*}\right\}dx^{*}\right]dh_{0}^{*} \tag{25}$$

For T^{*} , $H^{*}=h_{0}^{*}+A\{1-\cos(\pi x^{*})\}$.

Using the numerical method of integration, the film pressure (22), the load capacity (24) and the elapsed time (25) can be calculated.

3. Results and Discussions

On the squeeze film characteristics between cosine form convex curved plates surface roughness, porosity and transverse magnetic field effect is noticed. The squeeze film characteristics are presented for different values of dimensionless parameters specifically Hartman number M_0 , roughness parameter C and permeability parameter ψ .

By giving values to parameter C roughness effect on the bearing surfaces can be seen. The case $C \to 0$, the analysis reduces to that of absolutely smooth bearing surfaces. It is expected that for smaller values of C , the bearing characteristics are also not likely prominent. A range of figures plotted here reveal a link among smooth and roughness of the bearing surfaces, magnetic and nonmagnetic field cases and porous and non-porosity of material.

3.1. Squeeze film pressure

The pressure distribution variation P^{*} versus horizontal coordinate x^{*} for various M_0 values is shown in figures 2,3. As M_0 increases pressure increases in the fluid film area. The lubricant velocity of the plates decreases because of magnetic field effect and the sidewise fluid outflow is decreased because of surface asperities of the bearing surface, hence great quantity of fluid accumulates. Thus extra pressure is supplied in the boundary films.

3.2. Load carrying capacity

Figures 4,5 shows the variation of load capacity W^{*} against amplitude ratio A for different values of M_0 when all other parameters held stable. From these figures increment in load capacity is noticed for increased M_0 values compared to $M_0 = 0$. For roughness parameter C with permeability parameter ψ change in load capacity is seen in figure 6. Mean load capacity falls because of ψ for all values of C , whereas mean load capacity raises with raise in C . The obvious cause for this to occur is that better value of ψ leads to added empty space on the porous face, letting the fluid to get into the porous area. From the pores fluid flows away.Therefore trim down of fluid amount in the film area is noticed that leads to lessen pressure production and load capacity. Though, this considerable fall in load capacity could be compensated by appropriate values of roughness parameters and can be regained. This is clear from figure 7 and remarkable to note that for all values of M_0 , the load capacity increases gradually for the first few values of ψ and for some values of ψ , it further increases before starts to decrease for increasing ψ . Because of porousness, reduction in load capacity for all C and M_0 values is observed.

3.3. Non-dimensional Squeeze film time

For different M_0 values a graph of squeeze film time T^* versus squeeze film height h_0^* is plotted keeping other physical parameters constant shown in figure 8,9.Experientially squeezing time decreases as the film height increases. Also it is worth to mention that magnetic field effect is clearly seen. As magnetic parameter increases the squeeze film time also increases. Much fluid retains in the film region due to applied magnetic field which sturdily resists the flow. Thus, the squeezing time increases significantly disclosing the fact that the magnetic field offers the delayed squeeze film of the plates. We expect the similar results for roughness parameters that also increase the squeeze time which is not shown here for brevity.

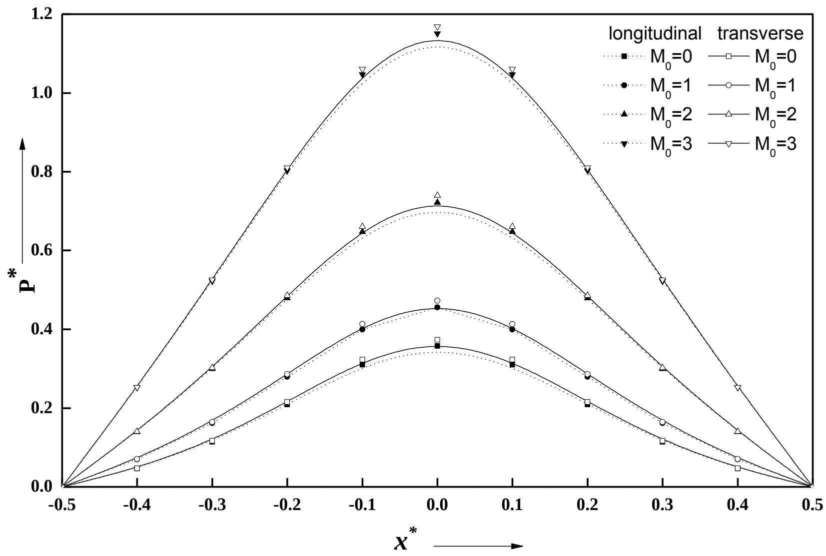

Fig.2. Variation of non-dimensional P^* with x^* for different values of M_0 with $\delta = 0.01$ and $C = 0.3$

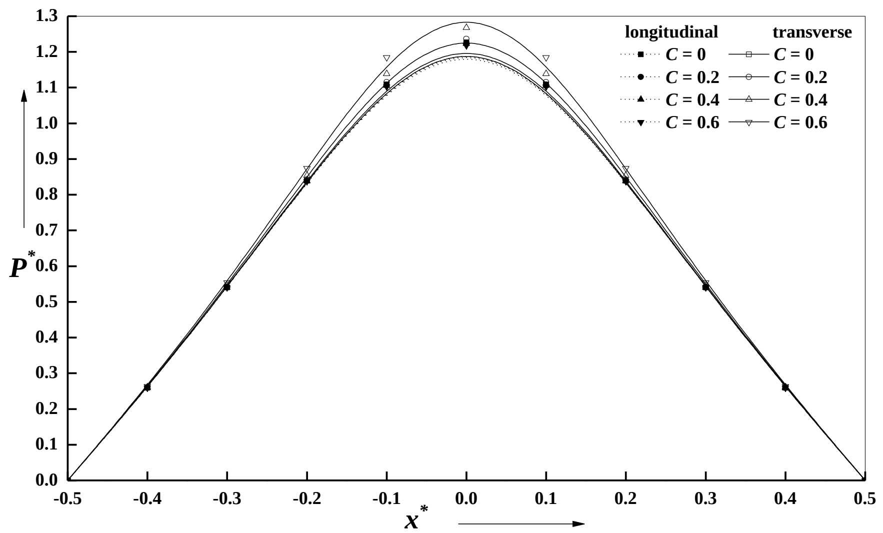

Fig.3. Variation of non-dimensional P^* with x^* for different values of C with $M_0 = 3$, $\delta = 0.01$ and $A = 1.5$

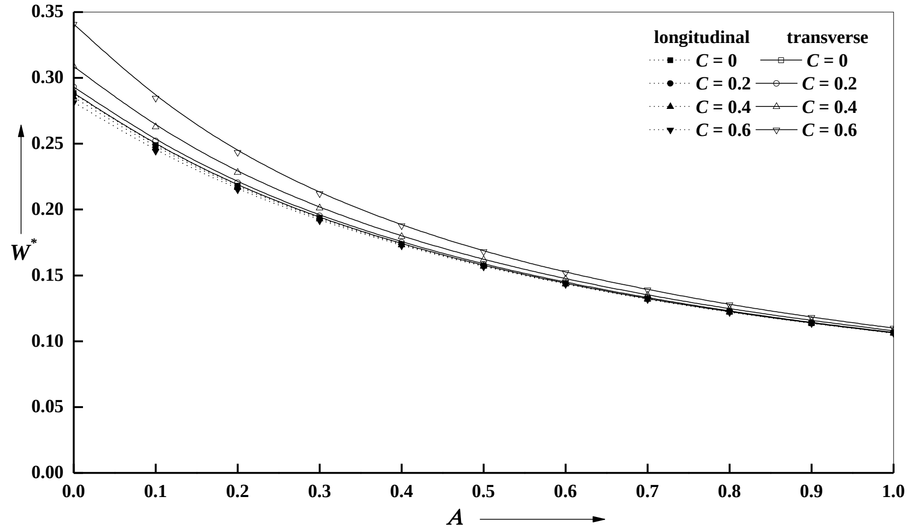

Fig. 4. Variation of non-dimensional W^* with A for different values of C with $M_0 = 3$, $\delta = 0.01$ and $\psi = 0.01$

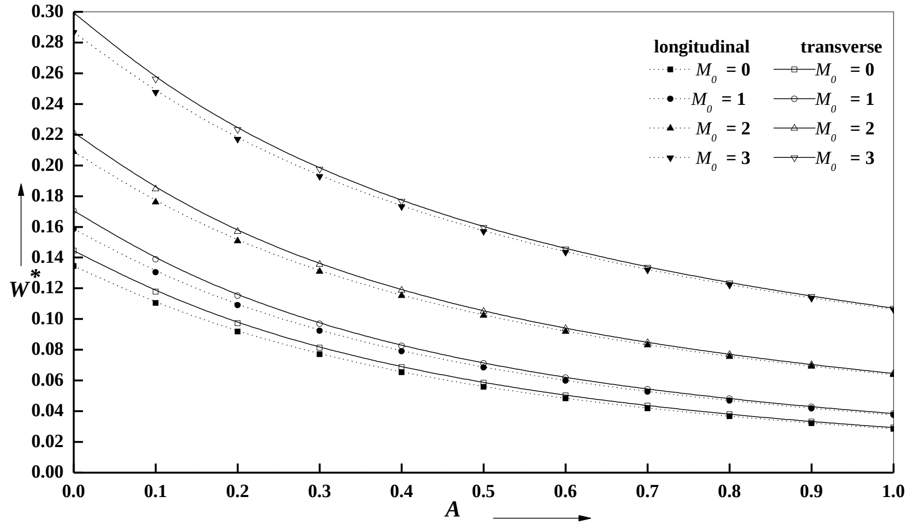

Fig. 5. Variation of non-dimensional W^* with A for different values of M_0 with $C = 0.3$, $A = 1.5$ and $\psi = 0.01$

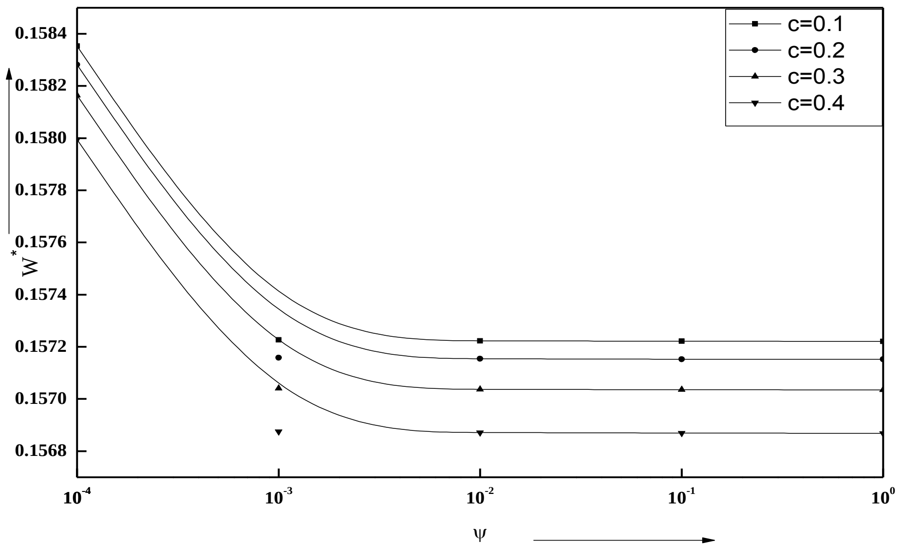

Fig.6. Variation of non-dimensional W^* with permeability parameter ψ for different values of roughness parameter C with $M_0 = 3, \delta = 0.01, A = 0.5$

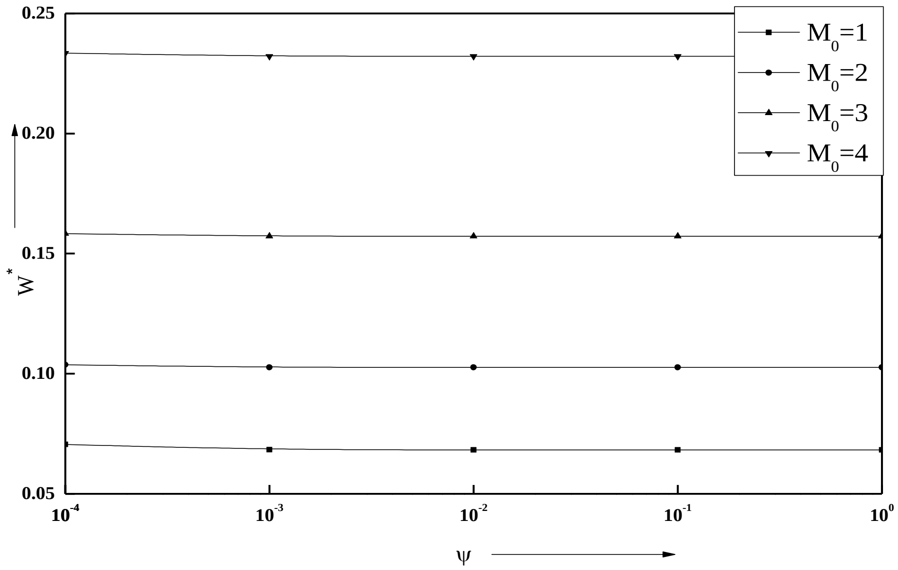

Fig.7. Variation of non-dimensional W^* with permeability parameter ψ for different values of M_0 with roughness parameter $C = 0.1,\ \delta = 0.01, A = 0.5$

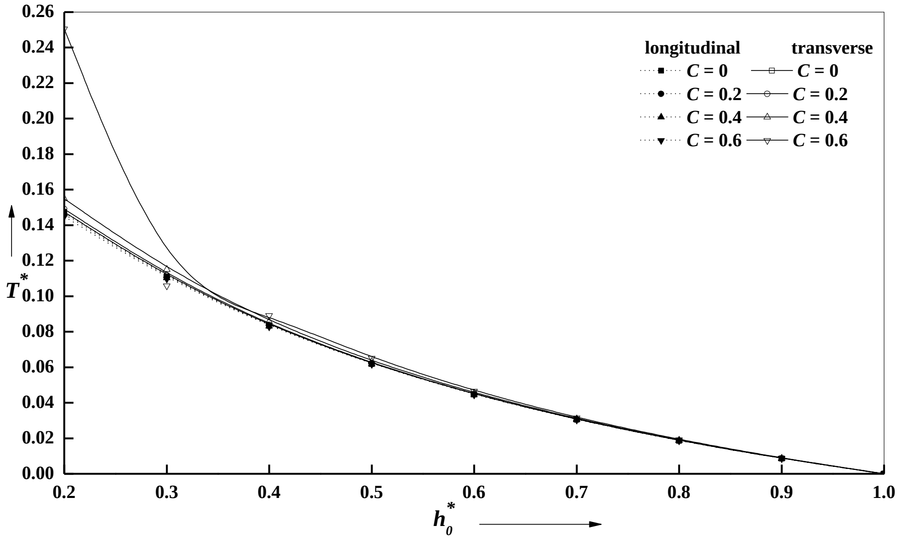

Fig. 8. Variation of non-dimensional T^* with h_0^* for different values of C with $M_0 = 3$, $A = 1.5$ and $\psi = 0.01$

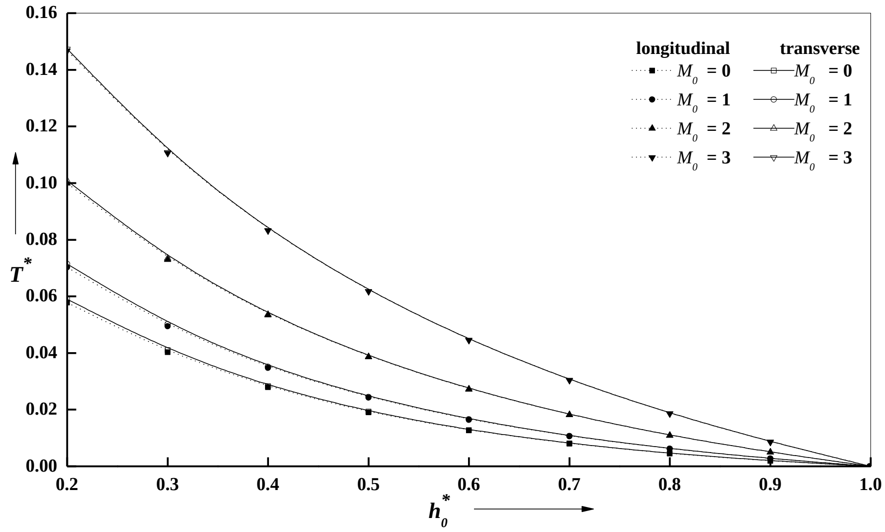

Fig. 9. Variation of non-dimensional T^* with h_0^* for different values of M_0 with $C = 0.3$, $A = 1.5$ and $\psi = 0.01$

The variation of R_{W^*} and R_{T^*} with M_0 is shown in Table 1 for increasing values of C. By the comparative percentage variation transverse magnetic field effect on the squeeze film characteristics is calculated. Increment in the dimensionless load carrying capacity R_{W^*} and dimensionless squeeze film time R_{T^*} are given by $R_{W^*} = \left\{ \dfrac{\left(W^*_{magnetic} - W^*_{non-magnetic}\right)}{W^*_{non-magnetic}} \right\} \times 100$, $R_{T^*} = \left\{ \dfrac{\left(T^*_{magnetic} - T^*_{non-magnetic}\right)}{T^*_{non-magnetic}} \right\} \times 100$.

Table1: Variation of R_{W^*} and R_{T^*} with M_0 for different values of C with $A=1.5$ and $\psi = 0.01$

		Longitudinal		Transverse	
		R_{W^*}	R_{T^*}	R_{W^*}	R_{T^*}
$M_0=0$	$C=0.1$	−0.1586	−1.4329	0.51199	2.9832
	$C=0.2$	−0.66972	−5.4787	2.08454	13.1617
	$C=0.3$	−1.5157	−11.4875	4.83318	35.8517
$M_0=1$	$C=0.1$	−0.1012	−1.35008	0.45579	2.92066
	$C=0.2$	−0.4626	−5.1678	1.85480	12.8827
	$C=0.3$	−1.0409	−10.8511	4.29870	35.0804
$M_0=2$	$C=0.1$	−0.0486	−1.13664	0.34909	2.7486
	$C=0.2$	−0.1848	−4.3637	1.42024	12.118
	$C=0.3$	−0.4086	−9.20507	3.28817	32.9689
$M_0=3$	$C=0.1$	−0.0146	−0.86646	0.26168	2.5073
	$C=0.2$	−0.0591	−3.3476	1.06301	11.0454
	$C=0.3$	−0.1354	−7.1268	2.45699	30.0055

4. Conclusion

Based on the stochastic theory of Christensen for irregular surfaces the characteristics of MHD squeeze-film amid cosine form convex curved plates with porosity and surface roughness shows the following conclusions drawn by above results

i. For both longitudinal and transverse roughness patterns an improvement in capacity of load carrying and time of response is noticed with transverse magnetic field which is applied externally.

ii. The roughness regarding the surface causes a reasonable effect on the characteristics concerning the bearing. Due to raise in surface roughness, huge amount of load is carried in the bearing and also response time of squeeze-film motion extends compared to the smooth case.

iii. In the limiting case, as $C \to 0$ for one-dimensional cosine form convex curved plates the result for both roughness patterns can be reduced to smooth surface case.

iv. The permeability of the porous covering reduces the squeeze-film characteristics as compared to the nonporous contention. As permeability increases pressure distribution,load carrying capacityand response time decreases.

Compared to the corresponding classical cases increase in permeability leads to decrease in the pressure distribution, load-carrying capacity, and squeeze time whereas these are found to increase for increasing values of roughness parameter and Hartmann number. These physical quantities increases bearing life and also giving suitable values to improve the working of the bearing.

References

[1] D.F. Hays, Squeeze films for rectangular plates, *ASME Journal of Basic Engineering*, *85*, 1963, 243-246.

[2] P.R.K. Murti, Squeeze films in curved circular plates, *ASME Journal of Lubrication Technology, 97*,1975, 650-652.

[3] O. Pinkus, and B. Sternlicht, *Theory of hydrodynamic lubrication* (McGraw Hill, New York, 1961).

[4] J.R. Lin, Pure squeeze film behavior in a hemispherical porous bearing using the Brinkman model, *STLE Tribology Transactions, 39*, 1996, 769-778.

[5] B.J. Hamrock, *Fundamentals of fluid film lubrication*(McGraw Hill, New York 1994).

[6] J.R. Lin, W.H. Liao, and C.R. Hung, The effects of couple stresses in the squeeze film characteristics between a cylinder and a plane surface, *Journal of Marine Science and Technology,12*,2004,119-123.

[7] J.R. Lin, Squeeze film characteristics between a sphere and a flat plate: couplestress fluid model, *Computers and Structures,75*, 2000, 73-80.

[8] C. Barus, Isothermals, iopiestics, and iometrics rlative to viscosity, *American Journal of Science,45*,1893,87-96.

[9] R.F. Lu, and J.R. Lin, A theoretical study of combined effects of non newtonian rheology and viscosity-pressure dependence in the sphere-plate squeeze-film system, *Tribology International,40*,2007,125-131.

[10] E.R. Maki, D. C. Kuzma, and R.L. Donnelly, Magnetohydrodynamic lubrication flow between parallel plates, *Journal of Fluid Mechanics*, *26(3)*, 1966, 537–543.

[11] M. I. Anwar and C. M. Rodkiewicz, Non uniform magnetic field effects in MHD slider bearing, *Journal of Lubrication Technology*, *94(1)*, 1972, 101–105.

[12] N. C. Das, Study of optimum load capacity of slider bearings lubricated with power law fluids, *Tribology International,32(8)*, 1999, 435–441.

[13] S. Kamiyama, Magnetohydrodynamic journal bearing (report 1), *Journal of Lubrication Technology*, *91(3)*,1969, 380–389.

[14] M. Malik and D. V. Singh, Analysis of finite magnetohydrodynamic journal bearings, *Wear*, *64(2)*, 1980, 273–280.

[15] J. B. Shukla, Hydromagnetic theory for squeeze films, *Journal of Basic Engineering*, *87 (1)*, 1965, 142–144.

[16] E. A. Hamza, Magnetohydrodynamic effects on a fluid film squeezed between two rotating surfaces, *Journal of Physics D*, *24(4)*, 1991, 547–554.

[17] N. M. Bujurke and R. B. Kudenatti, MHD lubrication flow between rough rectangular plates, *Fluid Dynamics Research*, *39(4)*, 2007, 334–345.

[18] H.Wu, Analysis of the squeeze film between porous rectangular plates, *Journal of Lubrication Technology*, *94(1)*, 1972,64–68.

[19] J. Prakash and S. K. Vij, Load capacity and time-height relations for squeeze films between porous plates, *Wear*, *24(3)*, 1973, 309–322.

[20] U. Srinivasan, The analysis of a double-layered porous slider bearing, *Wear*, *42(2)*, 1977 , 205–215.

[21] R. S. Gupta and V. K. Kapur, Centrifugal effects in hydrostatic porous thrust bearings, *Journal of Lubrication Technology*, *101(3)*, 1979, 381–392.

[22] N. B. Naduvinamani, S. T. Fathima, and S. Jamal, Effect of roughness on hydromagnetic squeeze films between porous rectangular plates, *Tribology International*, *43(11)*, 2010, 2145–2151.

[23] H. Christensen, Stochastic models for hydrodynamic lubrication of rough surfaces, *Proceedings of the Institution of Mechanical Engineers*, *184*, 1969, 1022–1033.

[[24] H. Christensen and K. Tønder, Tribology of rough surfaces, parametric study and comparison of lubrication models, *SINTEF Research Report No. 22/69-18* , 1969.

[25] L. S. H. Chow and H. S. Cheng, The effect of surface roughness on the average film thickness between lubricated rollers, *Journal of Lubrication Technology*, *98(1)*, 1976, 117–124.

[26] N. Patir and H. S. Cheng, An average flow model for determining effects of three-dimensional roughness on partial hydrodynamic lubrication, *Journal of Lubrication Technology*, *100(1)*,1978,12–17.

[27] N. M. Bujurke andN. B.Naduvinamani, A note on squeeze film between rough anisotropic porous rectangular plates, *Wear*, *217(2)*, 1998,225–230.

Appendix
Notation

B_0 applied magnetic field in the $z-$direction
c maximum asperity deviation from the nominal film height
C dimensionless roughness parameter (c/h_0)
H film thickness

L length of the plates
d amplitude of the cosine function
b width of the curved plates
A dimensionless amplitude ratio of the cosine function
h_0 minimum film thickness
h_0^* dimensionless film thickness after time Δt
h_s stochastic film thickness
k permeability of the porous matrix
p hydrodynamic film pressure
p^* pressure in the porous region
M_0 Magnetic Parameter $\left(=B_0 h_0 (\frac{\sigma}{\mu})^{1/2}\right)$
u, w Velocity components in film region
u^*, w^* Velocity components in porous region
x, y, z local Cartesian co-ordinates
m porosity
P^* dimensionless pressure $\left(=\frac{ph_0^3}{\mu L^2(-dH/dt)}\right)$
t mean time of approach
T^* Dimensionless time of approach $\left(=\frac{h_0^2 Wt}{\mu L^3 b}\right)$
V Squeezing Velocity $\left(-\frac{dH}{dt}\right)$
W^* Dimensionless load carrying capacity $\left(=\frac{h_0^3 W}{\mu L^3 b(-dH/dt)}\right)$

Greek symbols

σ Conductivity of fluid
μ lubricant viscosity
ξ random variable
$\bar{\sigma}$ standard deviation
ψ non dimensional permeability parameter
δ porous layer thickness
δ^* non dimensional porous layer thickness

